NRL Report 6556

A Finite Electronic Partition Function From Screened Coulomb Interactions

CARL A. ROUSE

E. O. Hulburt Center for Space Research
Atmosphere and Astrophysics Division

and

Space Sciences Laboratory
University of California
Berkeley, California

September 15, 1967

APPROVED FOR PUBLIC RELEASE - DISTRIBUTION UNLIMITED

NAVAL RESEARCH LABORATORY
Washington, D.C.

This page intentionally left blank.

CONTENTS

Abstract	iv
Problem Status	iv
Authorization	v
INTRODUCTION	1
NUMERICAL SOLUTIONS OF THE SCHRÖDINGER EQUATION WITH THE COMPLETE SCREENED COULOMB POTENTIAL	2
Method of Solution	2
Quantum Numbers from the Complete Screened Coulomb Potential	4
Approximate Analytic Fits to CSCP Quantum Numbers	8
A FINITE ELECTRONIC PARTITION FUNCTION	9
Normalization of Bound-State Wave Functions	9
Definition of a Finite Electronic Partition Function	11
Discussion	15
SUMMARY AND CONCLUSIONS	19
ACKNOWLEDGMENTS	20
REFERENCES	20
APPENDIX - The Meaning of the So-Called "Maximum Bound Principal Quantum Number"	23

ABSTRACT

A study was made of the problem of a finite partition function for bound electronic states in a hydrogenic ion and the associated problems of the intensity drop of spectral lines and the lowering of the effective ionization potential. Solutions of the Schrödinger equation (SE) with the complete screened Coulomb potential (CSCP) were obtained for 1s, 2s, 2p, 3s, 3p, and 3d states. The CSCP used is given by

$$V(r) \begin{cases} V_i(r) = -Ze^2\left(\frac{1}{r} - \frac{1}{D+A}\right), & 0 \leqq r \leqq A \\ V_0(r) = -Ze^2 \frac{D}{D+A} \frac{\exp[(A-r)/D]}{r}, & r \geqq A \end{cases}$$

where D is the screening radius and A is the mean minimum radius of the ion atmosphere. The standard transformations $x = 2Zr/\lambda a_0$ and $E_\lambda = -Z^2\mu e^4/2\hbar^2\lambda^2$, where λ is the CSCP quantum number, yield the well-known form of the SE with λ in place of n. The numerical solutions of the SE are obtainable using a nonlinear method that is accurate and stable. The resulting quantum numbers can be accurately described by simple analytic fits for a wide range of the interesting values of D. For a given ratio of A to D the relative normalizations of the CSCP wave functions to the corresponding Coulomb wave functions $\Phi_{n,\ell}(\lambda)$ can also be described by simple analytic functions. It was shown that for states where $3a_0n^2/2Z \approx D$, Φ is generally near $1/e$ for solutions with $A = D$. For $3a_0n^2/2Z > D$, Φ decreases rapidly. This Φ-function is used in the definition of a finite electronic partition function as a multiplying factor for each Boltzmann factor, viz., $\Phi_{n,\ell}(\lambda)\exp(-E_\lambda/kT)$. This is shown to be analogous to the definition of the equilibrium probability of a state derived by Tolman in his study of nonisolated systems. The problem of the number of screened Coulomb states was resolved: the CSCP yields as many states as the Coulomb potential. However, with the CSCP, for states with $3a_0n^2/2Z > D$, the separation of the levels is less than the corresponding Coulomb levels, i.e., the density of states near the continuum increases. Removal of ℓ-degeneracy, the question of a maximum bound principal quantum number, and integer quantization of the ground state quantum numbers was discussed. In particular, relative to various calculations of a maximum bound principal quantum number by perturbation and/or variational methods, it was shown that these methods actually calculate the increase in the energies of the states with small n, where $3a_0n^2/2Z < D$, by the amount $\Delta E \approx Ze^2/(D+A)$. Present results also apply to the unsolved problem of the intensity drop of hydrogen lines in the solar atmosphere and in laboratory hydrogen at a low temperature, where the observations are in excellent agreement with the CSCP solutions with $A = D/2$ and the effective screening radius is identified with the radius of the mean atomic volume. It was possible to calculate the observed ionization potential of hydrogen and to give evidence of a screened Coulomb red shift in laboratory spectra.

PROBLEM STATUS

This is a report of the work accomplished to date on the problem; work on other phases of the problem continues.

AUTHORIZATION

NRL Problem A01-02
Project RR 004-02-42-5300
Sponsored jointly by the Office of Naval Research
and the National Science Foundation

Manuscript submitted February 23, 1967.

A FINITE ELECTRONIC PARTITION FUNCTION FROM SCREENED COULOMB INTERACTIONS

INTRODUCTION

The standard electronic partition function (p.f.) for bound states is given by

$$Q_{eb} = \sum_{i,j} \exp(-E_{i,j}/kT), \tag{1}$$

where the $E_{i,j}$ are the energies of the bound states. From Coulomb interactions for a hydrogenic ion (neutral hydrogen will be an "ion" with zero charge),

$$Q_{eb} = \sum_{n} 2n^2 \exp(-E'_n/kT), \tag{2}$$

where n is the principal quantum number (q.n.); $2n^2$ represents the degeneracies of the states, and E'_n is the energy of the state relative to the ground-state energy taken as zero, i.e., $E'_n \sim 1-(1/n^2)$.

Unfortunately, Eq. (2) diverges as $n \to \infty$. Attempts to limit Q_{eb} have ranged from applications of the concepts of excluded volumes by Urey and Fermi (1) to the calculation of a maximum bound principal quantum number (2), with the region between filled with various ad hoc models (3) including recent attempts to count the number of bound states (4).

Since these approaches avoid the basic problem of calculating the eigenvalues for bound states (except for slight perturbations) of even the simple hydrogenic ion, it seemed interesting to consider numerical solutions of the Schrödinger equation (SE) with the complete screened Coulomb potential (5) as a well-established first-order interaction of a bound electron and its surrounding particles — essentially, the rest of the universe. In spite of remarks to the contrary (4), the eigenvalue problem turned out to be regular and the quantum numbers and relative normalizations of the wave functions can be accurately represented by simple analytic expressions. In the present report the definition of a finite electronic p.f. will be associated with the relative normalization of the bound states as a function of the screening distance. Since $[\psi_{n,\ell}(r)]^2$ represents the relative probability of finding the electron in state (n,ℓ) with energy $E_{n,\ell}$ between r and $r+dr$, then $\int[\psi_{n,\ell}(r)]^2 dr$ represents a relative total probability of finding the electron in state (n,ℓ). Now, if $[\psi_{n,\ell}(r,D)]^2$ changes upon introduction of an interaction potential with screening radius D, then the relative total probability of the state (n,ℓ) also changes as a function of D. Consequently, the ratio of the relative total probability with finite screening to that with infinite screening (the standard Coulomb solutions) will be referred to as the relative normalization — or relative probability — of the state.

The concepts and results introduced in this derivation will be applied to the unsolved problem of the intensity drop of hydrogen lines in the solar atmosphere and laboratory spectra. In addition, the problem of the change in ionization potential will be solved simultaneously.

Next, we will discuss numerical solutions of the Schrödinger equation with the complete screened Coulomb potential where consideration of the so-called "maximum bound principal quantum number" is given in the Appendix.

The finite electronic partition function will then be developed, from the correct normalization of the bound state, as the total probability of the state, and the results will be applied to the problem of the disappearance of hydrogen lines as well as to the problem of the observed ionization potential of hydrogen.

NUMERICAL SOLUTIONS OF THE SCHRÖDINGER EQUATION WITH THE COMPLETE SCREENED COULOMB POTENTIAL

The standard form of the complete screened Coulomb potential (CSCP) is given (5-7) by

$$V(r) \begin{cases} V_i(r) = -\dfrac{Ze^2}{\eta_0}\left(\dfrac{1}{r} - \dfrac{1}{D+A}\right), & 0 \le r \le A \\[2ex] V_0(r) = -\dfrac{Ze^2}{\eta_0}\,\dfrac{D}{D+A}\,\dfrac{\exp[(A-r)/D]}{r}, & r \ge A, \end{cases} \tag{3}$$

where D is the screening length, A is the mean minimum radius of the ion atmosphere (8,9) and η_0 is the dielectric constant of the medium, considered uniform everywhere.

For the present study we chose the Yukawa or Debye-Huckel (D-H) form of the screened Coulomb potential in Eq. (3), for two reasons. First, it has a simple analytic form and second, the work of Broyles et al. (10) indicates that a D-H radial distribution of charged particles is physically representative. Hence, potentials due to charged-particle distributions similar to the D-H radial distribution will lead to quantitative, but not qualitative, variations of the present results.

It will be assumed that values of D and A for a material of interest at a given density and temperature are derivable from other considerations. For example, in a low-density gas, the D-H screening radius is given by

$$D^2_{\text{D-H}} = kT\Big/\left(\eta_0 4\pi e^2 \sum_j N_j Z_j'^2\right), \tag{4}$$

where N_j is the number density of ions of kind j with charge Z_j'. In a degenerate Fermi gas D is proportional to k_F, where k_F is the Fermi momentum (11) divided by $\hbar$. In a solid or liquid D would probably be close to the radius of the mean atomic value (11) r_0. In various radial distributions of particles, one would expect values of A to range from $A \approx 0$ to $A \approx D$, where, in general, D corresponds to the mean distance to the maximum deviation from the average charge density of the medium. We consider values of A given by $A = 0$, $A = D$, and $A = D/2$ with $\eta_0 \equiv 1.0$ everywhere. The case with $A = 0$ corresponds to the situation with $V(r) = V_0(r)$ alone (with $A = 0$), the case usually considered in the literature by approximate perturbation or variational methods (2,3,12).

Method of Solution

After the standard transformations (13)

$$x = 2Zr/\lambda a_0 \tag{5}$$

and

$$E_\lambda = -\frac{Z^2\mu e^4}{2\hbar^2}\,\frac{1}{\lambda^2} \tag{6}$$

the radial SE for a hydrogenic ion with the CSCP given by Eq. (3) with $\eta_0 = 1.0$ becomes

$$\frac{d^2R}{dx^2} + \frac{2}{x}\frac{dR}{dx} - \left[\lambda v(x) + b^2 + \frac{\ell(\ell+1)}{x^2}\right] R = 0 \tag{7}$$

with

$$v(x) \begin{cases} v_i(x) = -\left(\frac{1}{x} - \frac{1}{d+a}\right), & 0 \le x \le a \\ v_0(x) = -\frac{d}{d+a}\,\frac{\exp[(a-x)/d]}{x}, & x \ge a, \end{cases} \tag{8}$$

where d and a are the values of D and A in x-space, and b^2 is a constant to be designated. In the standard analytic Coulomb solutions, $b^2 = 1/4$.

The numerical method of solution to Eq. (7) is that developed by the author (14) and will only be outlined for subsequent references. The wave function $R(x)$ and the slope of the wave function $m(x) = dR/dx$ are simultaneously expanded in a Taylor series, between space steps, to the cubic terms, viz:

$$R(x+\Delta x) = R(x) + m(x)\Delta x + \frac{1}{2}m'(x)\Delta x^2 + \frac{1}{6}m''(x)\Delta x^3 \tag{9}$$

and

$$m(x+\Delta x) = m(x) + m'(x)\Delta x + \frac{1}{2}m''(x)\Delta x^2 + \frac{1}{6}m'''(x)\Delta x^3, \tag{10}$$

with

$$m'(x) = -\frac{2}{x}m(x) + \left[b^2 + \frac{\ell(\ell+1)}{x^2} + \lambda v(x)\right] R(x), \tag{11}$$

from which $m''(x)$ and $m'''(x)$ can be obtained and $v(x)$ is given by Eq. (8). Note that in Eq. (9), $m'(x)$, and all higher derivatives are known exactly from the SE, but $R(x)$ and $m(x)$ are only available from the Taylor expansions in the previous step.

Exact initial values are obtained from a series solution of the SE and are applicable to all Coulomb and screened Coulomb wave functions. We write the series solution in the form

$$R(x) = x^\ell \phi(x), \tag{12}$$

with

$$\phi(x) = \Sigma \alpha_k x^k, \quad \alpha_0 \neq 0. \tag{13}$$

Letting (i) indicate the ith derivative, the initial values are given by

$$R^{(i)}_{\lambda,\ell}(0) \equiv i!\,\alpha_{i-\ell}, \tag{14}$$

where $\alpha_{i-\ell} = 0$ for $i < \ell$. From the series solution the α's are equal to

$$\alpha_1 = -\frac{\lambda}{2(\ell+1)}\alpha_0 \tag{15}$$

and

$$\alpha_{t+1} = \frac{b^2\alpha_{t-1} - \lambda\alpha_t}{(t+1)(2\ell+2+t)} \ , \quad t \geq 1 \ , \tag{16}$$

with

$$b^2 = \frac{1}{4} + \frac{\lambda}{d+a} \ . \tag{17}$$

In the present work all numerical results are carried out with $\alpha_0 = 1.0$ for $i = \ell$. Other values of α_0 will be considered, in the third part of the report, through analytical considerations.

It should be noted that in the region $x \leq a$, the series is exact for a given value of λ. For a large, say a greater than 20, this series solution essentially represents an accurate solution to the screened Coulomb problem. However, the CSCP q.n. λ would still have to be obtained by iterations in order to determine the value that would yield an exponential tail at large x.

Quantum Numbers from the Complete Screened Coulomb Potential

We now present the quantum numbers and, of course, eigenvalues obtained from numerical solutions of the SE with the CSCP. As described in Refs. 5 and 14, solutions were sought for wave functions with the same shapes as the Coulomb wave functions — i.e., the same number of nodes. Consequently, we will use the standard Coulomb designations $R_{n,\ell}$ for the corresponding CSCP wave functions with n and ℓ, the standard Coulomb principal q.n. and angular momentum q.n., respectively. The CSCP q.n. λ will be a function of d and a as well as n and ℓ. We will refer to the 1s, 2s, 2p, etc., states and/or wave functions with screening distance $d(D)$ and minimum ion atmosphere radius $a(A)$. The CSCP q.n.'s, λ, will also be written as $\lambda_{n,\ell}$, and it will be understood that

$$\lambda \equiv \lambda_{n,\ell} \equiv \lambda_{n,\ell}(d,a) \ . \tag{18}$$

The eigenvalues will all be given in units of rydbergs divided by Z^2, or from Eq. (6),

$$\epsilon_\lambda \equiv \frac{E_\lambda \, 2\hbar^2}{Z^2 \, \mu e^4} = -\frac{1}{\lambda^2} \ . \tag{19}$$

From Eq. (6)

$$\frac{ZD}{a_0} = \frac{\lambda d}{2} \tag{20}$$

as the transformation to r-space of the values of d assumed in Eqs. (7) and (8).

We consider the 1s, 2s, 2p, 3s, 3p, and 3d states with $a = d$, $a = 0$, and $a = d/2$. (The d in 3d will not be confused with the distance d.) We use space steps $\Delta x = 10^{-2}$ and $\Delta x = 10^{-3}$ to obtain four or more significant figure accuracy as was obtained in the linear study (5) with $\Delta x = 10^{-4}$. With $a = 0$, it was found necessary to use $\Delta x = 10^{-3}$ to obtain this desired accuracy. The maximum values of x used ranged from 10 to 25, as discussed in Ref. 14. All calculations were done on the CDC 3800 computer at the Naval Research Laboratory. With the linear system of equations previously analyzed, the automatic search for one

q.n. took about 12 to 15 min on a CDC 3600 computer using $\Delta x = 10^{-4}$. With the present cubic system of equations, q.n.'s can be calculated in about 4 to 5 min — including printer time — using $\Delta x = 10^{-2}$.

Tables 1, 2, and 3 present the CSCP q.n.'s for cases $a = d$, $a = 0$, and $a = d/2$, respectively. Table 4 presents more detailed information from solutions in which $ZD \approx 3a_0 n^2/2$. Note the decreases by a factor of about e in the eigenvalues and radial probability densities $x^2 R^2_{\lambda,\ell}$ below the values from the corresponding Coulomb wave function for solutions with $a = d$. (Also see Ref. 5.) The change in $x^2 [R_{\lambda,\ell}(x)]^2$ will be discussed in more detail in part three in relation to the relative probability of the state $\Phi_{n,\ell}(\lambda)$ shown in the last column. Figures 1, 2, and 3 present plots of λ vs d, $\log \lambda$ vs $\log (ZD/a_0)$, and ϵ_λ vs ZD/a_0, respectively.

Table 1
CSCP Quantum Numbers $\lambda_{n,\ell}$ from Solutions with $a = d$ for the 1s, 2s, 2p, 3s, 3p, and 3d States

d $(a = d)$	λ_{1s}	λ_{2s}	λ_{2p}	λ_{3s}	λ_{3p}	λ_{3d}
10^3	1.0010	2.0040	2.0040	3.0090	3.0090	3.0090
10^2	1.01005	2.0404	2.0404	3.0910	3.09135	3.09135
48	—	—	—	3.1930	3.1933	3.19335
32	—	2.1289	2.1289	—	—	—
24	—	—	—	3.3980	3.3983	3.39835
16	1.06445	2.2656	2.2656	—	—	—
12	1.0868	2.3609	2.3609	3.8420	3.8422	3.8423
9	—	—	—	4.1600	4.1608	4.16175
8	1.1328	2.5611	2.56135	—	—	—
6	1.1804	2.7717	2.7733	4.8273	4.8354	4.8468
4	1.2795	3.2113	3.2234	—	—	—
3	1.3824	3.6619	3.6973	6.8820	6.9754	7.1257
2	1.5941	4.5707	4.6887	—	—	—
1	2.2445	7.2872	7.8401	—	—	—
0.5	3.5556	—	—	—	—	—

Table 2
CSCP Quantum Numbers $\lambda_{n,\ell}$ from Solutions with $a = 0$ for the 1s, 2s, 2p, 3s, 3p, and 3d States

d $(a = 0)$	λ_{1s}	λ_{2s}	λ_{2p}	λ_{3s}	λ_{3p}	λ_{3d}
10^3	1.0020	2.0080	2.00795	3.0179	3.0179	3.0179
10^2	1.0199	2.07925	2.07963	3.1790	3.1790	3.1790
48	—	—	—	3.3660	3.3670	3.3721
24	—	—	—	3.7165	3.7250	3.7424
16	1.1219	2.4778	2.4907	—	—	—
12	—	—	—	4.39375	4.4240	4.4852
9	—	—	—	4.8335	4.8836	4.9856
8	1.2394	2.9301	2.9756	—	—	—
6	—	—	—	5.6951	5.7959	6.0019
4	1.4671	3.7998	3.9524	—	—	—
3	1.6168	—	—	8.2067	8.5237	9.1718
2	1.9083	5.4823	5.9602	—	—	—
1	2.7693	8.7716	10.149	—	—	—
0.5	4.4663	—	—	—	—	—

Table 3
CSCP Quantum Numbers $\lambda_{n,\ell}$ from Solutions with $a = d/2$ for the 1s and 2s States Only, with $\lambda_{2s}/2$ also Shown

d $(a = d/2)$	λ_{1s}	λ_{2s}	$\lambda_{2s}/2$
10^3	1.00133	2.0053	1.00265
10^2	1.01342	2.0540	1.0270
32	—	2.1736	1.0868
30	1.045	—	—
16	1.0868	2.3606	1.1803
8	1.1798	2.7589	1.37945
4	1.3746	3.5632	1.7816
3	1.5061	—	—
2	1.7692	5.1306	2.5653
1	2.5524	8.1936	4.0968
0.5	4.1044	—	—

Table 4
Details of CSCP Solutions where $ZD \approx 3a_0 n^2/2$ and CP is the Coulomb Potential*

State	V	d	a	$\lambda_{n,\ell}$	$(xR)^2_{max}$	$(xR)^2_{x=d}$	ZD/a_0	$\Phi_{n,\ell}(\lambda)$
1s	CP	—	—	1.0000	0.54134	0.44808†	—	1.0000
	CSCP	1.802	1.802	1.6648	0.1979‡	0.1681	1.5000	1.3933
	CSCP	1.214	0.0	2.4676	0.1063	0.1016	1.4978	0.2764
2s	CP	—	—	2.0000	0.38187	0.35694	—	1.0000
	CSCP	3.55	3.55	3.3819	0.1360	0.1289	6.0030	0.3772
	CSCP	2.483	0.0	4.8332	0.08221	0.08217	6.0004	0.2866
2p	CP	—	—	2.0000	4.68880	3.21246	—	1.0000
	CSCP	3.55	3.55	3.4014	0.5670	0.3946	6.0374	0.3630
	CSCP	3.509	3.509	3.4200	0.5551	0.3911	6.0004	0.3597
3s	CP	—	—	3.0000	0.30460	0.30238	—	1.0000
	CSCP	5.3	5.3	5.0974	0.1079	0.1076	13.508	0.3728
3p	CP	—	—	3.0000	1.37405	1.26514	—	1.0000
	CSCP	5.3	5.3	5.1114	0.1658	0.1543	13.545	0.3650
3d	CP	—	—	3.0000	115.649	65.5850	—	1.0000
	CSCP	5.3	5.3	5.13175	4.657	2.654	13.599	0.3526

*The relative normalization $\Phi_{n,\ell}$ is discussed in part three of this report.
†CP results at $3n^2/2 = Z\bar{r}_n/a_0$.
‡Maximum value printed out.

Figure 3 deserves additional comment. The plots of $(\epsilon_{n,\ell} - \epsilon_{1s})$ vs ZD/a_0 in this figure have the well-known shapes associated with the lower part of the spread of the electronic energy levels in the conventional band theory of solids. Note that for $A = D$ the decrease in the separation of the levels occurs only when $ZD/a_0 < 3n^2/2$. For $ZD/a_0 \gtrsim 3n^2/2$ the separations of the levels are essentially equal to the separations of the corresponding Coulomb levels. Obviously, with a net positive screening as one would expect for an electron either bound to a negative ion or interacting with "holes" (positrons), similar calculations would lead to a variation similar to the upper part of the solid-state band of energy levels. Finally, if a bound electron experiences a net negative screening for large

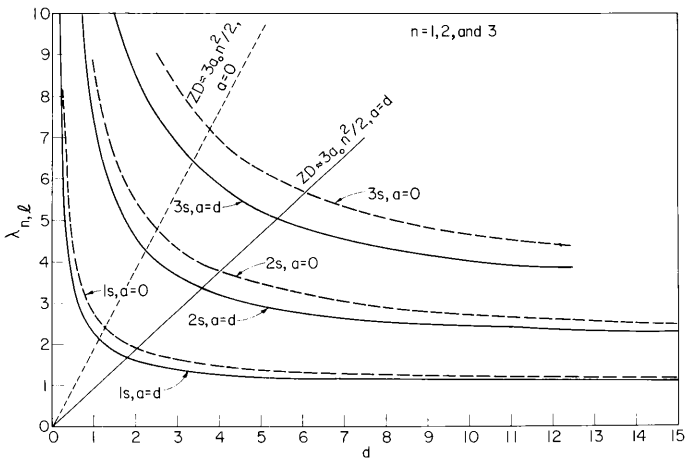

Fig. 1 - $\lambda_{n,\ell}$ vs d from CSCP solutions with $a = d$ and $a = 0$ for 1s, 2s, and 3s states. The solid straight line connects the origin with points where d = 1.8, 3.6, and 5.4 on the $a = d$ curves for 1s, 2s, and 3s states, respectively. The dashed straight line connects similar points with d = 1.25, 2.5, and 3.75 on the $a = 0$ curves. Note that, generally, for either solution with $a = d$ or $a = 0$, a line through the origin connects points with $d(n, s) \approx nd(1, s)$, as shown for $d(1, s)$ = 1.8 and 1.25. The relation is almost exact for lines near and to the right of the ones shown for the $a = d$ and $a = 0$ solutions.

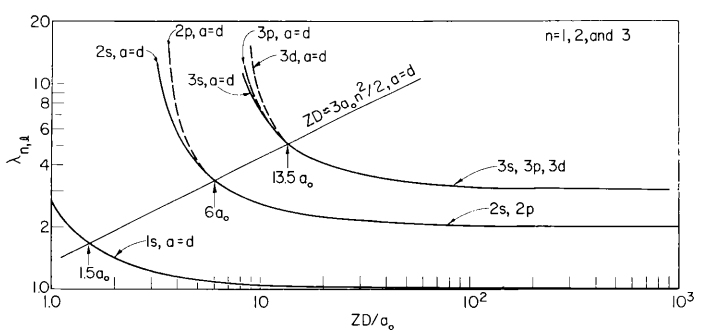

Fig. 2 - Log $\lambda_{n,\ell}$ vs log ZD/a_0 from CSCP solutions with $a = d$ for 1s, 2s, 2p, 3s, 3p, and 3d states. The straight line connects points where $ZD \approx 3a_0n^2/2$. See Fig. 1. $ZD/a_0 = \lambda d/2$, with $\lambda_{n,\ell}$ from Tables 1 and 4.

screening distances, and a net positive screening for small screening distances, then it would be expected that, as r_0 decreases, the energy of a level relative to the ground state would first decrease, then increase as exhibited qualitatively in conventional solid-state theory. This will be considered quantitatively in a later study.

With the present hydrogenic CSCP solutions the parts of the $(\epsilon_{n,\ell} - \epsilon_{1s})$ curve labeled with $n \geq 2$, $n \geq 3$, etc., represent "bands" of bound states. From left to right, the part with

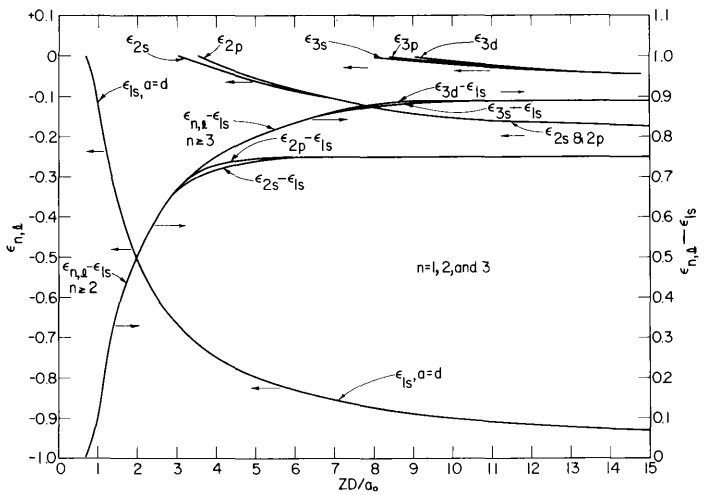

Fig. 3 - $\epsilon_{n,\ell}(\lambda)$ vs ZD/a_0 and $[\epsilon_{n,\ell}(\lambda) - \epsilon_{1s}(\lambda)]$ vs ZD/a_0 from CSCP solutions with $a = d$ for 1s, 2s, 2p, 3s, 3p, and 3d states. $\epsilon_{n,\ell}(\lambda) = -1/\lambda^2_{n,\ell}$, with $\lambda_{n,\ell}$ from Table 1.

$ZD/a_0 \lesssim 3$, labeled $n \geq 2$, represents the merging of all excited states. The portion between $3.3 \lesssim ZD/a_0 \lesssim 7$, labeled $n \geq 3$, represents the merging of all excited states with $n \geq 3$. Clearly, the extension beyond $ZD/a_0 \gtrsim 8$, but less than about 14 or 15, would represent the merging of excited states with $n \geq 4$, and so on. And, of course, the bona fide continuum would lie above this $(\epsilon_{n,\ell} - \epsilon_{1s})$ band.

Approximate Analytic Fits to CSCP Quantum Numbers

When this study was started, it was expected that definite patterns would be found in the values of the q.n.'s. A simple analytic fit to the q.n.'s, valid over the range of interest for this study, is given for s-states by

$$\frac{\lambda_{n,s}}{n} \approx 1 + Cw - \left[\left(1 - \frac{2a}{d}\right) e^{-w}(0.525w^2 + 0.14w^3)\right], \tag{21}$$

with

$$w = \frac{n}{d} \lesssim 1.0, \qquad 0 \leq a \leq d,$$

$$C = C_1 = 2\Big/\left(1 + \frac{a}{d}\right), \quad w \lesssim \frac{1}{12},$$

and

$$C = C_2 = 2\left(1 - \frac{a}{2d}\right), \quad w \gtrsim \frac{1}{12}.$$

For other ℓ-states, Eq. (21) also gives $\lambda_{n,\ell}$ accurately for $D \gtrsim 3a_0 n^2/2Z$, which is about the same range above for $\lambda_{n,s}$. A more general analytic fit to the present CSCP quantum numbers appears to be possible by an expression of the form

$$\frac{\lambda_{n,\ell}(a,d)}{n} = 1 + Cw + \sum_{j=2}^{J} B_j(n,\ell,d,a)\, w^j e^{-(w/j-1)},$$

where w and C are defined in Eq. (21). For three-digit accuracy in the range $w \lesssim 1$, only two terms are needed in the summation to $J = 3$. However, in the range $w \lesssim 10$, four terms are needed to $J = 5$. For example, in the 1s state with $a = d$ and $w \leqq 10$, values of the B_j's are given by B_2 = 0.525, B_3 = 0.080, B_4 = 0.0040, and B_5 = 0.000132. A slight increase in the B_j's as a function of n and ℓ will lead to fits to the other values of $\lambda_{n,\ell}(a = d)$ in Tables 1 and 4. (Note: $\lambda_{1s}(a = d = 0.1 = 14.056)$.) The values of $\lambda_{n,\ell}(a = 0)$ can be fitted by either another set of constants, or simply by the $a = d$ expression but with a negative sign in front of the summation.

The solutions with $a = d/2$ established the C-fits in Eq. (21), with the term in brackets indeed nearly dropping out, except for $w \gtrsim 1$. Actually, C_2 is a "good" fit over the entire range, but C_1 is better for $w < 1/12$.

Note that s-state quantization occurs in whole number multiples of the ground state only for $a \approx d/2$ and for fixed values of w. But for $w \ll 1$, integer quantization occurs for all $0 \leqq a \leqq d$ to a high degree of accuracy for fixed $w = n/d$.

Note further from Tables 1 and 2 and Fig. 3 that, to three significant figures or so, the eigenvalues (quantum numbers) for states with $\ell > 0$ are not significantly different from solutions with $A = D$ until the screening distance is less than $3a_0n^2/2Z = \bar{r}_n$, the mean position of the electron in the corresponding Coulomb (n, s) state. (See also Table 4.)

For a specific application the quantum numbers (eigenvalues) from the CSCP can be calculated more accurately, and more accurate fits can be derived. For the present general study of the SE with the CSCP the above fits will suffice.

In closing this section, we see that for $d > 0$, the CSCP yields an eigenfunction for all Coulomb n, ℓ. Consequently, there are at least as many CSCP states as there are Coulomb states. But for states with $D < \bar{r}_n$ the spacings between levels are significantly less than those of the corresponding Coulomb states. (And for solutions with $A = 0$ this decrease occurs for values of D greater than $\bar{r}_n$.) Now, since there is no explicit "maximum bound principal quantum number" (see the Appendix), this is how the CSCP and the Coulomb potential yield the same number of states: with the CSCP the density of states near the continuum increases!

Having presented an outline of the numerical method and some solutions of the CSCP, we proceed to the basic statistical mechanical problem of a finite partition function for the bound electronic states.

A FINITE ELECTRONIC PARTITION FUNCTION

How can screened Coulomb interactions of bound electrons be used to define a finite p.f.? We have shown that the CSCP and Coulomb potential yield the same number of bound states (infinite), there being no such quantity as an explicit "maximum bound principal quantum number." What the CSCP solutions yield that may be useful is the total probability of the state, which varies with changes in d and a. In what follows, spin degeneracy will be omitted, since it is well known to be 2.

Normalization of Bound-State Wave Functions

Before presenting the CSCP results, it will be necessary to derive the correct transformation of the radial normalization integral from x-space to r-space. The desired r-space normalization integral — the total probability of the state — is given by

$$\int_0^\infty r^2 [R_{n,\ell}(r)]^2 \, dr = 1 \tag{22}$$

for the normalized radial wave functions $R_{n,\ell}(r)$. But what is usually evaluated is (13)

$$\int_0^\infty x^2 [R_{n,\ell}(x)]^2 \, dx = N(n,\ell) \, . \tag{23}$$

Then $N(n,\ell)$ is multiplied by $(a_0 n/2Z)^3$ to obtain this value for the unnormalized wave function in r-space, or,

$$\int_0^\infty r^2 \left[R_{n,\ell}\left(\frac{2Zr}{na_0}\right)\right]^2 dr = \left(\frac{a_0 n}{2Z}\right)^3 N(n,\ell) \, . \tag{24}$$

However, for any radial wave function of the form $x^s \phi(x)$, we substitute $R_{n,\ell}(x) = x^\ell \phi_{n,\ell}(x)$ into Eq. (23) and obtain

$$\int_0^\infty x^{2\ell+2} [\phi_{n,\ell}(x)]^2 \, dx = N(n,\ell) \, , \tag{25}$$

where $s = \ell$. From Eq. (5), $x = 2Zr/na_0$ and $dx = 2Zdr/na_0$, hence, the transformation of the left side of Eq. (25) yields

$$\int_0^\infty r^{2\ell+2} \left[\phi_{n,\ell}\left(\frac{2Zr}{na_0}\right)\right]^2 dr = \left(\frac{a_0 n}{2Z}\right)^{2\ell+3} N(n,\ell) \tag{26}$$

as the correct transformation (with $\lambda = n$ in Eq. (5) for all n and ℓ). In other words, the standard normalized analytic Coulomb radial wave functions, when handled correctly, should be

$$R_{n,\ell}(r) = - \left\{\left(\frac{2Z}{a_0 n}\right)^{2\ell+3} \frac{(n-\ell-1)!}{2n[(n+\ell)!]^3}\right\}^{1/2} e^{-x/2} x^\ell L_{n+\ell}^{2\ell+1}(x) \, , \tag{27}$$

where $L_{n+\ell}^{2\ell+1}(x)$ is the associated Laguerre polynomial.

With the numerical solution for the CSCP, the present normalization integrals are carried out by the Trapezoidal Rule to $x = x_{max}$. In Ref. 14 it is shown that this yields very accurate answers. Hence, for our study, we can approximate

$$\int_0^{x_{max}} x^{2\ell+2} [\phi_{\lambda,\ell}(x)]^2 \, dx \approx N(\lambda, \ell, d, a) \, , \tag{28}$$

which can easily be made as accurate as one desires (14).

Now, for a given ℓ and a, $N(\lambda, \ell, d, a)$ decreases as $d \to 0$. For d and/or $a \to \infty$, $N(\lambda, \ell, d, a) \to N(n, \ell)$, the normalization integral for the corresponding Coulomb wave function. Next, since initial magnitudes can be arbitrary, the present numerical calculations were all carried out with initial magnitudes equal to 1.0 for s-states, initial slopes equal to 1.0 for p-states, etc. This is equivalent to setting $\alpha_0 = 1.0$ in the series solution, Eq. (13) — even for Coulomb wave functions. (In Ref. 5, it is demonstrated that all Coulomb s-states yield identical normalizations if modified to have the same initial values.)

The final modification of the normalization integral is one that is necessary to give relative values of $r^2[R_{\lambda,0}(r)]^2$ in r-space proportional to $x^2[R_{\lambda,0}(x)]^2$ calculated in x-space for s-states. It is shown in Ref. 5 that this will be true for s-states if the initial magnitude of the wave function is $1/\lambda$ in r-space. The equivalent series in r-space would have $a_0 = 1/\lambda$. Consequently, the net effect on the magnitude of the normalization, Eq. (28), would be to divide the right side by λ^2. Therefore, the presently desired transformation of $N(\lambda, \ell, d, a)$ calculated in x-space leads to

$$\int_0^\infty r^{2\ell+2}\left[\phi_{\lambda,\ell}\left(r;\frac{1}{\lambda}\right)\right]^2 dr = \left(\frac{a_0}{2Z}\right)^{2\ell+3} \lambda^{2\ell+1} N(\lambda, \ell, d, a). \tag{29}$$

In the present CSCP solutions, for a given ℓ and a, as $d \to 0$, $\lambda^{2\ell+1}N(\lambda) \to 0$ also. Or, $N(\lambda)$ decreases faster than $\lambda^{2\ell+1}$ increases.

Definition of a Finite Electronic Partition Function

The right side of Eq. (29) describes the total probability of an hydrogenic state that has the "arbitrary" constant of the wave function set equal to $1/\lambda$, where λ is the CSCP quantum number for the state. And, since the change from a Coulomb state to a screened Coulomb state reflects the interaction of a bound electron with the external particles of the ion atmosphere, the relative normalization of the screened Coulomb state could possibly be of interest in expressing the increased probability that the bound electron in the n, ℓ-state will interact with a neighboring particle or particles — or, a decreasing probability of finding an electron in that state because of the increased probability of being perturbed. Since the screening of interest depends on the time-averaged positions of the neighboring particles, the mean effect on a system of particles could be expressed by a modification of the Boltzmann factor; or, we define — for a given D and A —

$$Q_{eb}^{\text{CSCP}} = 2\sum_{n,\ell} \Phi_{n,\ell}(\lambda, D, A)\ \exp(-E_\lambda/kT), \tag{30}$$

where $\Phi_{n,\ell}$ is a function of the relative normalization of the CSCP wave function to the corresponding Coulomb wave function.

From Eq. (29) we define

$$\Phi_{n,\ell}(\lambda, D, A) = \frac{\lambda^{2\ell+1} N(\lambda, \ell)}{n^{2\ell+1} N(n, \ell)} \tag{31}$$

for a radially symmetric potential.* As mentioned above, whenever we write λ alone, the dependence on D and A is implied. Tables 5, 6, and 7 give values of $\Phi_{n,\ell}(\lambda)$ for the cases

*Note added in proof: The reader's attention is called to the fact that the basic theoretical argument used to derive the probability $\Phi_{n,\ell}$ is that the electron charge probability density should change under screening. This phenomenon appears to be measurable through the isomer shift (where the nucleus emits a gamma ray) with the Mössbauer effect. Note the following published reports: O.C. Kistner, and A.W. Sunyer, Phys. Rev. Letters 4:412 (1960); S. DeBenedetti, G. Lang, and R. Ingalls, Phys. Rev. Letters 6:60 (1961); L.R. Walker, G.K. Wertheim, and V. Jaccarino, Phys. Rev. Letters 6:98 (1961); J.H. Wood, Phys. Rev. 117:714 (1960); D.N. Pipkorn, C.K. Edge, P. Debrunner, G. De Pasquali, H.G. Drickamer, and H. Frauenfelder, Phys. Rev. 135:A1604 (1964); R. Ingalls, Phys. Rev. 155:157 (1967); R. Ingalls, H.G. Drickamer, and G. De Pasquali, Phys. Rev. 155:165 (1967); J.-P. Bocquet et al. Phys. Rev. Letters 17:809 (1966); H.S. Möller, and R.L. Mössbauer, Phys. Letters 24A:416 (1967).

Table 5
Relative Normalizations $\Phi_{n,\ell}(\lambda)$ from CSCP Solutions with $a = d$ for 1s, 2s, 2p, 3s, 3p, and 3d States and $ZD/a_0 = \lambda d/2$, with $\lambda_{n,\ell}$ from Table 1

d $(a = d)$	1s		2s		2p		3s		3p		3d	
	ZD/a_0	Φ_{1s}	$ZD/4a_0$	Φ_{2s}	$ZD/4a_0$	Φ_{2p}	$ZD/9a_0$	Φ_{3s}	$ZD/9a_0$	Φ_{3p}	$ZD/9a_0$	Φ_{3d}
10^3	500	0.998	250	0.996	250	0.996	167	0.993	167	0.993	167	0.994
10^2	50.50	0.980	25.5	0.961	25.50	0.961	17.17	0.943	17.17	0.941	17.17	0.942
48	—	—	—	—	—	—	8.515	0.884	8.515	0.882	8.515	0.882
30	15.15	0.935	8.016	0.875	8.017	0.875	—	—	—	—	—	—
24	—	—	—	—	—	—	4.531	0.781	4.531	0.779	4.531	0.779
16	8.516	0.882	4.531	0.779	4.531	0.778	—	—	—	—	—	—
12	6.521	0.847	3.541	0.718	3.541	0.718	2.561	0.611	2.561	0.610	2.561	0.610
9	—	—	—	—	—	—	2.080	0.524	2.080	0.522	2.081	0.521
8	4.531	0.779	2.561	0.608	2.561	0.611	—	—	—	—	—	—
6	3.541	0.718	2.079	0.526	2.080	0.523	1.609	0.405	1.612	0.399	1.616	0.390
4	2.559	0.615	1.606	0.409	1.611	0.398	—	—	—	—	—	—
3	2.074	0.534	1.373	0.335	—	—	1.147	0.253	1.163	0.236	1.188	0.206
2	1.594	0.421	1.143	0.250	1.172	0.219	—	—	—	—	—	—
1	1.122	0.257	0.911	0.147	0.980	0.104	—	—	—	—	—	—
0.5	0.889	0.146	—	—	—	—	—	—	—	—	—	—

Table 6
Relative Normalizations $\Phi_{n,\ell}(\lambda)$ from CSCP Solutions with $a = 0$ for 1s, 2s, 2p, 3s, 3p, and 3d States and $ZD/a_0 = \lambda d/2$, with $\lambda_{n,\ell}$ from Table 2

d $(a = 0)$	1s		2s		2p		3s		3p		3d	
	ZD/a_0	Φ_{1s}	$ZD/4a_0$	Φ_{2s}	$ZD/4a_0$	Φ_{2p}	$ZD/9a_0$	Φ_{3s}	$ZD/9a_0$	Φ_{3p}	$ZD/9a_0$	Φ_{3d}
10^3	501	0.998	251	0.995	251	0.993	168	0.992	168	0.989	168	0.989
10^2	51.00	0.963	26.00	0.930	25.99	0.928	17.66	0.891	17.66	0.891	17.66	0.899
48	—	—	—	—	—	—	8.976	0.809	8.979	0.813	8.992	0.814
30	15.99	0.901	—	—	8.488	0.800	—	—	—	—	—	—
24	—	—	—	—	—	—	4.955	0.690	4.967	0.689	4.990	0.669
16	8.975	0.804	4.956	0.689	4.981	0.690	—	—	—	—	—	—
12	—	—	—	—	—	—	2.929	0.531	2.949	0.539	2.990	0.561
9	—	—	—	—	—	—	2.417	0.473	2.442	0.473	2.493	0.501
8	4.957	0.687	2.930	0.537	2.976	0.541	—	—	—	—	—	—
6	—	—	—	—	—	—	1.898	0.384	1.932	0.383	2.001	0.415
4	2.934	0.534	1.900	0.382	1.976	0.384	—	—	—	—	—	—
3	—	—	—	—	—	—	1.368	0.251	1.421	0.245	1.529	0.268
2	1.908	0.377	1.370	0.248	1.490	0.2395	—	—	—	—	—	—
1	1.385	0.242	1.096	0.150	1.268	0.1235	—	—	—	—	—	—
0.5	1.117	0.143	—	—	—	—	—	—	—	—	—	—

Table 7
Relative Normalizations $\Phi_{n,\ell}(\lambda)$ from CSCP Solutions with $a = d/2$ for 1s and 2s States and $ZD/a_0 = \lambda d/2$, with $\lambda_{n,\ell}$ from Table 3

d $(a = d/2)$	1s		2s	
	ZD/a_0	Φ_{1s}	$ZD/4a_0$	Φ_{2s}
10^3	501	0.997	251	0.995
10^2	50.67	0.974	25.67	0.948
32	—	—	8.694	0.847
30	15.68	0.915	—	—
16	8.694	0.847	4.721	0.719
8	4.719	0.721	2.759	0.545
4	2.749	0.551	1.782	0.381
3	2.259	0.478	—	—
2	1.769	0.379	1.283	0.248
1	1.276	0.238	1.024	0.149
0.5	1.026	0.138	—	—

$A = D$, $A = 0$ and $A = D/2$, respectively. Some of these values are plotted in Figs. 4 and 5 as a function of $u = ZD/a_0 n^2$. With the equivalence of $\alpha_0 = 1.0$ in the series solutions, Eq. (13), for the Coulomb wave functions, the exact normalization integrals for these wave functions, $N(n,\ell)$, are equal to 2, 2, 2, 24, 9, and 720 for the 1s, 2s, 3s, 2p, 3p, and 3d states, respectively. The approximate values obtained numerically for these Coulomb wave function normalizations (14) by the Trapezoidal Rule, integrating to $x_{max} = 20$ as in Eq. (28), are accurate to three or more significant figures.

The most interesting property of $\Phi_{n,\ell}$ is that for a given relationship between a and d, the function $\Phi_{n,\ell}$ is essentially independent of n and ℓ for $u = ZD/a_0 n^2 \gtrsim 2$. Furthermore, at $u = 1.5$ the spread in values of $\Phi_{n,\ell}$ for the states considered is only four units in the second significant figures, as is also shown in Table 4, last column. However, for larger values of n this spread at $u = 1.5$ may increase. But since the low-lying states are the most important for most applications, this relatively small spread is very convenient: it suggests the possibility of simple analytic fits. For example, for $u > 1.5$, $\exp(-1.5/u)$ falls in the upper part of the "Φ-band," and for $u < 1.5$, $\exp[-(1.5/u)^m]$, with $m \approx 2$ or 3, falls nicely in the lower part of the Φ-band. If, now, we substitute for u, the mean Φ-function can be approximated by

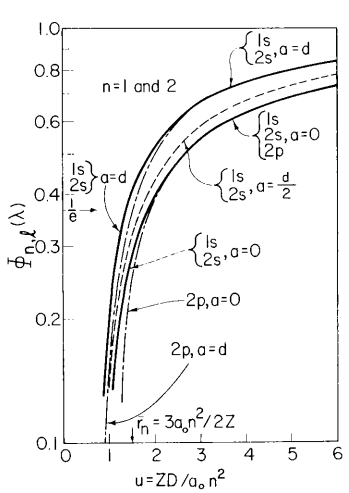

Fig. 4 - Log $\Phi_{n,\ell}(\lambda)$ vs $ZD/a_0 n^2$ from CSCP solutions with $a = d$, $d/2$, and 0, for 1s, 2s, and 2p states. The case $a = d/2$ is shown only for 1s and 2s states. Note $1/e \approx 0.368$. The mean position of an electron in a Coulomb s-state is $3a_0 n^2/2Z$. Hence, $u = 1.5$ is the mean position for all s-states. Note the small deviations of the p-state and d-state at $u = 1.5$.

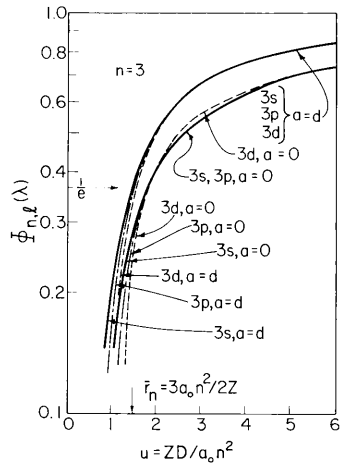

Fig. 5 - Log $\Phi_{n,\ell}(\lambda)$ vs ZD/a_0n^2 from CSCP solutions with $a = d$ and 0 for 3s, 3p and 3d states. The 3s solutions are near the 1s and 2s solutions shown in Fig. 4 even with $u \lesssim 1.5$. The 3d-curve with $a = 0$ was tested with more accurate calculations using $\Delta x = 10^{-4}$, but the 3 percent difference between $u = 2$ and 3 was not altered.

$$\Phi_{n,\ell}(\lambda, D, A) \approx \Phi_{n,\ell}(D) = \exp\left[-\left(\frac{1.5a_0n^2}{ZD}\right)^m\right] \tag{32}$$

with $m \approx 1$ for $D \gtrsim \bar{r}_n$, and $1 < m \lesssim 3$ for $D < \bar{r}_n$. Note that the relative probability of the state represented by $\Phi_{n,\ell}$ is generally decreased approximately by a factor of e for that state for which $ZD \approx 3a_0n^2/2$, i.e., when the screening distance is nearly equal to the mean position of the electron in the corresponding Coulomb s-state. For the case $a = d$, this is almost exactly true.

This latter observation suggests the CSCP interactions with $a = d$ yields the quantum analog of the semiclassical statistical mechanical "excluded volume" of Urey and Fermi (1). As derived by Fowler, the equivalent of Φ, call it p, is written as

$$p = \exp\left[-\left(\frac{a_0n^2}{r_0}\right)^3\right], \tag{33}$$

where r_0 is the radius of a mean volume for interactions associated with the free charged particles. Note here that the e-fold reduction in p occurs when $r_0 = a_0n^2$, the classical Bohr radius.

Discussion

In any system where the total sum over states — the complete partition function — can be separated into translational, electronic, vibrational, etc., states, the above definition of Q_{eb}^{CSCP}, the bound electronic contribution, is a natural generalization that reflects the first-order interaction of the bound electron with the surrounding particles. Tolman (15), in discussing the long-time behavior of nonisolated systems, derives an expression for the equilibrium probability P_n of finding any given state n with energy E_n, that is given by

$$P_n = \rho_{nn} = C e^{-\beta E_n}, \tag{34}$$

where ρ_{nn} is the density matrix, C and β are parameters having values independent of the state n, and the quantities E_n are the true energies for the various energy eigenstates n. Of course in equilibrium, $\beta = 1/kT$. Now, however, in the CSCP interactions of bound states, the relative normalization Φ represents a quantum analog of C in Eq. (34). Note

that with a given A, for bound states where $D > \bar{r}_n$, Φ is functionally independent of the state (n, ℓ), but the magnitude of Φ lies between 1 and about $1/e$ for a finite screening distance D. Furthermore, the Φ's cannot generally be normalized by setting $Q_{eb} = 1.0$. With systems of bound and free electrons in ionization equilibrium, normalization for all the possible electronic states, if necessary, would have to be relative to

$$Q_{eb}^{\mathrm{CSCP}} + Q_{ef}^{\mathrm{FD}} = 1, \tag{35}$$

where Q_{ef}^{FD} is the p.f. for free and/or mobile electrons satisfying Fermi-Dirac statistics. At high densities, mobile electrons behaving as "free" particles have a classical analog in that a particle acted upon by no external forces and a particle upon which the sum of the external forces is zero, behave in the same manner.

Clearly, the partition function for bound electronic states given by Eq. (30) does not contradict any basic statistical mechanics — it generalizes the previous definition to one that reflects the mean interaction of bound electrons with neighboring particles. And the present definition is based on solutions of the SE. We can summarize by saying that $\Phi_{n,\ell}(\lambda, D, A)$ represents the probability, relative to that for an isolated atom (ion), of an atom (ion) having an unperturbed, bound electronic state with energy E_λ when the bound electron interacts with neighboring particles via a screened Coulomb potential, the screened Coulomb potential being characterized by an effective screening distance D, by an effective mean minimum ion atmosphere radius A for the neighboring particles, and by a dielectric constant η for the first-order effect of neutral atoms or molecules. Here, of course, we have assumed $\eta \equiv 1.0$.

In studying matter at high temperatures and/or high or low densities, a finite electronic partition function is necessary in the analysis of all phenomena in which there is a significant probability that a bound electron can be excited and/or ionized. The magnitude of an electronic p.f. for bound electrons will, as discussed here, depend on the interactions experienced by bound electrons with neighboring particles, which essentially constitute the rest of the universe. In equilibrium phenomena the p.f. defined by Eq. (30) can be used as the bound electronic state contribution to the total sum over states in statistical mechanics. Although an hydrogenic ion was considered above, it is conceivable that the electronic states of diatomic atoms would also be influenced by a screened Coulomb potential in a qualitatively similar manner. In problems of astrophysical interest the description of a mixture of elements in ionization equilibrium at low to high densities ρ and at temperatures T greater than about 0.4 eV ($\approx 4000°$K) would be of interest. Also, the study of strong shock waves, exploding wires, plasmas, and other high-temperature phenomena could be described very reasonably by monatomic matter. Clearly, an accurate theoretical description of monatomic matter would have wide application. Such a formulation should be compatible with a formulation that considers diatomic molecules and then clusters of atoms that lead to the liquid and solid states (16) at lower temperatures, i.e., the condensation problem.

A description of matter — for either equation of state and/or opacity calculations, for example — based upon a modified Saha equation (17) with finite electronic p.f.'s provides such a theoretical formulation for monatomic matter at a given T and ρ applicable over a wide range of densities. The efforts of the author to develop an accurate and useful monatomic formulation have been reported elsewhere in the literature (18), as well as the applications to exploding wires (19) and stellar structure (20).

Applications of the standard Saha equation to opacity calculations are given by Stromgren (21) and in the article by Cox (22), and to equilibrium shock wave calculations by McChesney (23). However, at the higher densities, the modified Saha equation should be used.

Quantitative ionization equilibrium equation of state (IEEOS) calculations, with the refinements of the present report and with comparisons to results based upon the Thomas-Fermi-Dirac model of the atom (24), will be reported later. It will only be noted here that the basic postulates, in Refs. 17 and (20(b), are verified almost exactly in the present screened Coulomb solutions with $A = D$ and with the identification of the screening distance D with the radius of the mean atomic volume r_0 at high densities. This also applies to the density-dependent Coulomb wave functions in Ref. 17 as approximate CSCP wave functions.

Next, a more direct test of the CSCP effects is in the observations of relative intensities of lines similar to those reported by Ivanov-Kholodnyi and Nikol'skii (25,26) who report "... In prominence and chromospheric spectra, it has been found that near the series limit the lines do not merge because of broadening and convergence, but instead they disappear because of a rapid fall in intensity. As a result, we fail to observe the last few lines of the series, even though their half-widths are smaller than the separation between them." It has been shown (27) that this "rapid fall in intensity" is indeed compatible with the present relative normalizations when applied to the disappearance of hydrogen lines in the solar photosphere and the chromosphere — provided that, at low densities also, the effective screening distance is correlated with r_0 and with the present CSCP solutions with $A = D/2$. The correlation of r_0 with D at liquid or higher densities was expected (above and see Refs. 11, 17, and 20b), but this is the first known evidence for this correlation at low densities. As shown in Ref. 27, an effective maximum bound state n_e defined by

$$n_e^2 = 0.59\, ZD/a_0 \tag{36}$$

for the state where $\Phi \approx 1/e$ in solutions with $A = D/2$ is in excellent agreement with the last significantly occupied hydrogen levels in the solar atmosphere; the state where $\Phi \approx 0.1$ in solutions with $A = D/2$ is in excellent agreement with the last distinct levels observed in the solar atmosphere. The resulting relation for these maximum detected levels n_m is

$$n_m^2 = ZD/a_0 \,. \tag{37}$$

And, as expected, setting D equal to the Debye radius leads to very inaccurate answers.

Further evidence of the effect of screening on the disappearance of the Balmer lines of hydrogen even at very low temperatures — demonstrating a dominant density dependence — is in the experimental results of G. M. Shrum (28). With an electric discharge through nearly pure hydrogen at $T = 21°K$ and a pressure of 5 mm Hg, Shrum was just able to detect the H_{2-8} line in the Balmer series. Assuming that the pressure is given by $P = NkT$, N and r_0 can be determined. With this r_0 the maximum detected level is given by $n_m^2 = r_0/a_0$ and yields $n_m \approx 9.4$ or 9. Considering that the electric field acts as an additional perturbation and multipole interactions have not been included in the present calculations, this value represents a good agreement with observation. Next, we consider the calculation of the effective ionization potential for hydrogen to illustrate the lowering of an atom's ionization potential owing to screening. Since a depression of the continuum is equivalent to an increase in the energy of the ground state, let us consider the change in the ground-state energy. For $w \ll 1$, Eq. (21) yields

$$\begin{aligned} \frac{\lambda_{n,s}}{n} &\approx 1 + \frac{2d}{(d+a)}\,\frac{n}{d} \\ &= 1 + C_1 w \,. \end{aligned} \tag{38}$$

Now, the energy of state n is

$$E_{n,s}(\lambda) = -\frac{Z^2 \mu e^4}{2\hbar^2} \frac{1}{\lambda_{n,s}^2} . \tag{39}$$

Since $1 \leqq C \leqq 2$ in the physically interesting range, $C_1 w$ is also $<<1$. Substituting Eq. (38) into Eq. (39) and retaining the term linear in w,

$$E_{n,s} \approx -\frac{Z^2 \mu e^4}{2\hbar^2} \frac{1}{n^2} + \frac{Z\mu e^4}{\hbar^2} \frac{a_0}{(D+A)} \frac{\lambda}{n} . \tag{40}$$

Hence, the increase in the ground state energy is given by

$$\Delta E_{n,s} \approx \frac{Ze^2}{D+A} , \tag{41}$$

since $\lambda/n \approx 1$ for $Cw << 1$, and $(\hbar^2/a_0 \mu e^2) \equiv 1.0$. Consequently, for large screening distances, the energies of all states with small n are increased by $Ze^2/(D+A)$.

We now consider, explicitly, the energy change for the 1s state. The maximum detected levels of hydrogen in the solar chromosphere (29) are n_m = 38 to 40; this indicates that for n_m = 38, $r_0 = n_m^2 a_0$ = 1444 a_0. Substituting $D = r_0$ and $A = r_0/2$ into Eq. (41), one obtains

$$\Delta E_{1,s} = \frac{e^2}{1.5 r_0} = 1.256^{-2} \text{ eV} .$$

Then from Eq. (40),

$$E_{1,s}(n_m = 38) \approx -\frac{\mu e^4}{2\hbar^2} + \frac{e^2}{1.5 r_0} = -13.592 \text{ eV}.$$

For n_m = 40, similar calculations lead to a ground-state energy of

$$E_{1,s}(n_m = 40) = -13.594 \text{ eV} .$$

These values are to be compared to the recent calculations of Garcia and Mack (30) of the limiting hydrogen level using Dirac energies and a quantum-electrodynamical correction. Their value of E_{limit} = 109678.7642 cm^{-1}, converted to electron volts yields, relative to $E = 0$ at the continuum,

$$E_{1,s}(G-M) = -13.598 \text{ eV} .$$

Consequently, with respect to the accepted ionization potential for hydrogen of 13.595 eV, the Schrödinger equation with a screened Coulomb potential yields as accurate a value as the Dirac equation with a quantum-electrodynamical correction.

Another effect that would decrease the ionization potential is line broadening (6). However, the only quantitative change in Eq. (40) would occur relative to states near the continuum where the energy added during a perturbation would free the electron, i.e., perturb it to a positive energy state. Otherwise, broadening of states near the continuum limit — particularly for states with $\bar{r}_n >> D$ — can only lead to merging of states. These merged bound states still contribute to the p.f. even if only with diminishing effect because of the "guillotining" due to $\Phi_{n,\ell}$ in screened Coulomb interactions. Note that line broadening is completely consistent with the present results, since the neighboring particles that produce line broadening are the same particles whose time-averaged effect

leads to a screened potential. This includes neutral particles through multipole interactions, as well as charged particles.

Finally, as a test of the change in separation of the energy levels with screening, CSCP eigenvalues from solutions with $A = 0$, plotted as in Fig. 3, indicate that there indeed would be a decrease in the separation of the n = 2 - 3 levels — H_α line — even for $r_0/a_0 \approx 90$, the screening radius resulting above in the Shrum experiment. This is the correct sign of the change needed to calculate the observed wavelength of the H_α line of 6562.82 Å from the theoretical Coulomb SE H_α line of 6561.29 Å (allowing for refraction, of course). However, since the change is small (essentially zero for solutions with $A = D$), more accurate CSCP calculations with $A = D/2$ are necessary before presenting a value for this screened Coulomb red shift.

Other evidence of red shifts in laboratory spectra is found in observations of high-temperature plasmas (31). However, the shifts have been attributed to a quadratic Stark effect, where the theoretical values exceed the observed values by 20 percent. As indicated above, multiple interactions can be handled in a screened Coulomb potential through the dielectric constant, where preliminary calculations (9) have shown that an $\eta > 1.0$ would lead to a decrease in the present Φ-function relative to calculations with $\eta = 1.0$.

SUMMARY AND CONCLUSIONS

Some numerical solutions of the Schrödinger equation with the complete screened Coulomb potential (CSCP) have been presented with tables and graphs of quantum numbers $\lambda_{n,\ell}$ and relative normalizations $\Phi_{n,\ell}(\lambda)$. Although the SE with a screened Coulomb potential is not analytic, λ and Φ can be accurately described by simple, analytic functions for a wide range of interesting values of the screening distance D.

The problem of a maximum bound principal quantum number or a finite number of screened Coulomb states has been resolved: the screened Coulomb potential yields at least as many bound states as the Coulomb potential. For a CSCP wave function with the same shape as a Coulomb (n, ℓ) wave function, any $D > 0$ will yield a bona fide bound-state solution with a noninteger quantum number $\lambda_{n,\ell} > n$. However, with the CSCP, for states with $3a_0n^2/2Z > D$, the separation of the levels is less than the separation of corresponding Coulomb levels. In other words, the density of states near the continuum increases under screening. In addition, for states with $3a_0n^2/2Z > D$, the relative normalization $\Phi_{n,\ell}(\lambda)$ decreases very rapidly. The above results are used to define the quantum analog of the equilibrium probability of a state as derived by Tolman for a nonisolated system. This, of course, serves as the basis of a finite partition function for bound electronic states, which is based on solutions of the Schrödinger equation.

The concepts and results introduced here also resolve the problem of the intensity drop of hydrogen lines in the solar photosphere and chromosphere and in very low temperature hydrogen in laboratory measurements. The excellent agreement with the maximum effective bound state and the maximum detected levels in the solar atmosphere and the good agreement with the disappearance of Balmer lines in very low temperature hydrogen essentially confirm both the definition of the relative probability of an unperturbed state, derived here, and the fact that the effective screening radius is correlated with the radius of the mean atomic volume at low densities as well as at high densities. This implies that the electron clouds of the nearest neighbor atoms also contribute to the screening of bound states as do the free particles of the ion atmosphere. Hence, Debye-Hückel theory applied to plasmas is applicable only to ideal, charged, hard spheres or to point charges.

The effect of screening on the lowering of the ionization potential of an atom is illustrated by the calculation of the observed ionization potential of hydrogen as accurately as it is calculated by more elaborate methods.

In closing, astrophysical observations of effective maximum bound states and/or maximum distinct levels will enable one to calculate an ion-number density in the source of absorption or emission lines. This will be valuable in obtaining more information about the atmospheres of stars in general, and quasi-stellar objects (32) and X-ray sources (33) in particular, as well as local density variations in the atmosphere of the sun (34). And, of course, with a given relative abundance of elements, a mass density can be computed.

ACKNOWLEDGMENTS

This research was conducted while the author was an E. O. Hulburt Research Appointee supported by the Office of Naval Research and the National Science Foundation. I sincerely thank both organizations for the support that made this investigation possible.

I gratefully acknowledge the hospitality and assistance of the E. O. Hulburt Center staff. In particular, I wish to express my appreciation to Dr. Herbert Friedman for providing a pleasant and productive atmosphere for scientific research.

I also wish to thank Dr. Jerome Karle of NRL for helpful discussions and for reviewing the manuscript.

Finally, I wish to acknowledge the cooperation and assistance of the staff of the NRL Research Computation Center. Here, the programming of Mrs. Doris E. Gossett was of great value.

REFERENCES

1. Fowler, R.H., "Statistical Mechanics," Cambridge:Cambridge Univ. Press, 1936

2. Ecker, G., and Weizel, W., Ann. Physik 17:126 (1956); Margenau, H., and Lewis, M., Rev. Mod. Phys. 31:569 (1959); Harris, G.M., Phys. Rev. 125:1131 (1962); Ecker, G., and Kröll, W., Phys. Fluids 6:62 (1963); Smith, C.R., Phys. Rev. 134:A1235 (1964)

3. Armstrong, B.H., and Brush, S.G., "Opacity of High Temperature Air," Appendix in "Progress In High Temperature Physics and Chemistry," Vol. 1, C.A. Rouse, editor, New York: Pergamon (in press). This appendix gives "... a brief bibliography of theory and experiment regarding the effect of interactions with other particles on the ionization potential of an atom."

4. Schey, H.M., and Schwartz, J.L., Phys. Rev. 139:B1428 (1965)

5. Rouse, C.A., "Numerical Solutions of the Schrödinger Equation With the Complete Screened Coulomb Potential," Univ. of Calif. Lawrence Radiation Lab. (Livermore) Report 12101, Apr. 5, 1965

6. Margenau, H., and Lewis, M., in Ref. 2

7. Hill, T.L., "An Introduction To Statistical Thermodynamics," Reading, Mass.:Addison-Welsey, 1960

8. Rouse, C.A., "A Note On the Maximum Bound Principal Quantum Number," in "6th Int. Conf. on Ionization Phenomena in Gases," Paris, Vol. I, p. 225, 1963

9. Rouse, C.A., "Dependence of the Solutions of the Schrödinger Equation on the Dielectric Constant in the Complete Screened Coulomb Potential," Univ. of Calif. Lawrence Radiation Lab. (Livermore) Report 12461, Apr. 15, 1965

10. Broyles, A.A., Sahlin, H.L., and Carley, D.D., Phys. Rev. Letters 10:319 (1963)

11. Thouless, D.J., "The Quantum Mechanics of Many-Body Systems," New York and London:Academic, 1961

12. Meeron, E., "Statistical Mechanics of Reversible Processes in Plasma Dynamics," in "Plasma Physics," J.E. Drummond, editor, New York:McGraw-Hill, 1961

13. Schiff, L.I., "Quantum Mechanics," New York:McGraw-Hill, 1949; Bethe, H.A., and Salpeter, E.E., "Quantum Mechanics of One- and Two-Electron Atoms" and "Hb. d. Phys.," Vol. 33, Berlin:Springer-Verlag, 1957; Sherwin, C.W., "Introduction to Quantum Mechanics," New York:Holt, Rinehart and Winston, 1960; Leighton, R.B., "Principles of Modern Physics," New York:McGraw-Hill, 1959

14. Rouse, C.A., "Accurate and Stable Numerical Solutions to the Schrödinger Equation," Feb. 7, 1966; A.P.S. Bull. 11:356 (1966) J. of Math. and Phys. Vol. 46, p. 63, 1967

15. Tolman, R.C., "The Principles of Statistical Mechanics," Oxford:Oxford Univ. Press, 1938

16. Slater, J.C., "Quantum Theory of Molecules and Solids," Vols. 1 and 2, New York: McGraw-Hill, 1963 and 1965; Pines, D., and Nozières, P., "The Theory of Quantum Liquids," New York, Amsterdam:Benjamin, 1966

17. Rouse, C.A., "Ionization Equilibrium at High Densities," Ap. J. 139:339 (1964)

18. Rouse, C.A., (a) Ap. J. 134:435, 1961; (b) 135:599, 1962; (c) 136:636, 1962; (d) 136: 665, 1962; (e) 137:1286, 1963 (See also Refs. 8 and 17)

19. Rouse, C.A., "Theoretical Calculations of Exploding Wire Phenomena," Univ. of Calif. Lawrence Radiation Lab. (Livermore) Report 5684-T and APS Bull. 4:449 (1959)

20. Rouse, C.A., "Calculation of Stellar Structure Using an Ionization Equilibrium Equation of State," Univ. of Calif. Lawrence Radiation Lab. (Livermore) Report 7820, Rev. 1, July 20, 1964; Rev. 1, Supplement, Jan. 7, 1965; "New Solar Model," APS Bull. 10:14 (1965)

21. Strömgren, B., Zs. f. Ap. 4:118 (1932); See S. Chandrasekhar, "An Introduction to the Study of Stellar Structure," New York:Dover, 1957

22. Cox, A.N., "Stellar Absorption Coefficients and Opacities," in "Stars and Stellar Systems," Vol. VIII, L.H. Aller, and D.B. McLaughlin, editors, Chicago Univ. Press, 1965

23. McChesney, M., Can. J. Phys. 42:2473 (1964)

24. Brush, S.G., "Theories of the Equation of State of Matter at High Pressures and Temperatures," in "Progress In High Temperature Physics and Chemistry," Vol. I, C.A. Rouse, editor, Pergamon (in press)

25. Ivanov-Kholodnyi, G.S., Nikol'skii, G.M., and Gulyaev, R.A., Soviet Ast. - A.J. 4:754 (1961)

26. Ivanov-Kholodnyi, G.S., and Nikol'skii, G.M., Soviet Ast. - A.J. 5:339 (1961)

27. Rouse, C.A., Nature 212:803 (1966)

28. Shrum, G.M., Proc. Roy. Soc. A, 105:259 (1924); also note the observations of R.W. Wood (Roy. Soc. Proc. 97:455 (1920) who wrote, "If the pressure is gradually raised, the higher (Balmer) members disappear in succession, as they should on Bohr's theory."

29. Mitchell, S.A., Ap. J. 1051 (1947); Thomas, R.N., and Athay, R.G., "Physics of the Solar Chromosphere," New York:Interscience Publishers, Inc., 1961

30. Garcia, J.D., and Mack, J.E., J. Opt. Soc. Am. 55:654 (1965)

31. Berg, H.F., Ali, A.W., Lincke, R., and Griem, H.R., Phys. Rev. 125:199 (1962); Griem, H.R., Phys. Rev. 128:515 (1962)

32. Greenstein, J.L., and Schmidt, M., Ap. J. 140:1 (1964); Sandage, A., Ap. J. 141:1560 (1965); Burbidge, G.R., Burbidge, M., Hoyle, F., and Lynds, C.R., Nature 210:774 (1966)

33. Bowyer, S., Byram, E.T., Chubb, T.A., and Friedman, H., Science 147:394 (1965); Sandage, A.R., Osmer, P., Giacconi, R., Gorenstein, P., Gursky, H., Waters, J., Bradt, H., Garmire, G., Sreekantan, B.V., Oda, M., Osawa, K., and Jugaku, J., Ap. J. 146:316 (1966); Friedman, H., Byram, E.T., and Chubb, T.A., Science 153:1527 (1966)

34. Tousey, R., "The Extreme Ultraviolet Spectrum of the Sun," in "Space Science Reviews" 2:3 (1963)

APPENDIX

THE MEANING OF THE SO-CALLED "MAXIMUM BOUND PRINCIPAL QUANTUM NUMBER"

Clearly, for any $d > 0$ the CSCP will yield an eigenfunction for all Coulomb n, ℓ. One may inquire, then, about the exact meaning of the concept of a maximum bound principal quantum number (2-5,8).

If, now, one assumes that the spacing of all the CSCP levels are equal to the spacing of the Coulomb levels and also assumes that the continuum is depressed by ΔE_{1s} in Eq. (41), then there will be a level with, say, $n = g^*$, whose absolute magnitude will nearly equal ΔE_{1s} as in Ref. 8,

$$\left| - \frac{Z^2 \mu e^4}{2\hbar^2 g^{*2}} \right| \approx \frac{Ze^2}{D + A}$$

or,

$$g^{*2} = \frac{Z}{2a_0} (D + A), \tag{A1}$$

since $a_0 = \hbar^2/\mu e^2$. Consequently, the so-called maximum bound principal quantum number g^* is the fictitious CSCP q.n. for that level which would be at the edge of the continuum if the CSCP levels were all assumed spaced as the standard Coulomb levels and raised by an amount $\Delta E = Ze^2/(D + A)$ for large screening distances D.

It should be noted that Eqs. (41) and (A1) were derived in Ref. 8 from straightforward physical arguments, and it is the only reference, prior to the present study, to derive the correct dependence of g^* on A and D. It should also be noted that the basic pitfall in previous calculations of a "maximum bound principal quantum number" was the assumption that for a finite screening distance, there exists an eigenvalue equal to zero. Obviously, this assumption was made to explain the disappearance of spectral lines in plasmas. A more reasonable explanation for this is given in the text.

We will now demonstrate the difference in the "q.n." g^* for the edge of the continuum and the q.n. n_e of the state in which the relative probability $\Phi_{n,\ell}$ is about $1/e$. For $A = D$, g^* is given by Eq. (A1) as $g^{*2} = ZD/a_0$. Now for the state in which $n = n_e$, from Fig. 4 for s-states, $1.5\, a_0 n_e^2 \approx ZD$, or

$$\left.\begin{aligned} g^{*2} &= 1.0 \frac{ZD}{a_0} \\ n_e^2 &\approx 0.67 \frac{ZD}{a_0} \end{aligned}\right\} \text{ with } A = D, \tag{A2}$$

which are significantly different. At the other extreme, for $A = 0$, Eq. (A1) yields $g^{*2} = 0.5\, ZD/a_0$, whereas the state for which $\Phi \approx 1/e$ is, from Fig. 4, given by $1.85\, a_0 n_e^2 \approx ZD$ or

$$\left.\begin{aligned} g^{*2} &= 0.50\,\frac{ZD}{a_0} \\ n_e^2 &\approx 0.54\,\frac{ZD}{a_0} \end{aligned}\right\} \text{with } A = 0, \tag{A3}$$

which are surprisingly close in value. Finally, for $A = D/2$, from Eq. (A1) and Fig. 4,

$$\left.\begin{aligned} g^{*2} &= 0.75\,\frac{ZD}{a_0} \\ n_e^2 &\approx 0.59\,\frac{ZD}{a_0} \end{aligned}\right\} \text{with } A = D/2, \tag{A4}$$

where n_e^2 in (A4) is near the mean value of n_e^2 from Eqs. (34) and (A3). Consequently, in constructing an empirical partition function — which was the objective of Ecker and Weizel and others — a more meaningful principal quantum number with which to terminate the series is the whole number nearest n_e, or perhaps $n_e + 1$. The ℓ-states corresponding to n_e should also be included.

Security Classification

DOCUMENT CONTROL DATA - R & D

(Security classification of title, body of abstract and indexing annotation must be entered when the overall report is classified)

1. ORIGINATING ACTIVITY (Corporate author) Naval Research Laboratory Washington, D.C. 20360	2a. REPORT SECURITY CLASSIFICATION Unclassified 2b. GROUP

3. REPORT TITLE

A FINITE ELECTRONIC PARTITION FUNCTION FROM SCREENED COULOMB INTERACTIONS

4. DESCRIPTIVE NOTES (Type of report and inclusive dates) A report of the work accomplished to date on the problem; work on other phases continues.

5. AUTHOR(S) (First name, middle initial, last name)

Carl A. Rouse

6. REPORT DATE September 15, 1967	7a. TOTAL NO. OF PAGES 29	7b. NO. OF REFS 35
8a. CONTRACT OR GRANT NO. NRL Problem A01-02 b. PROJECT NO. RR 004-02-42-5300 c. d.	9a. ORIGINATOR'S REPORT NUMBER(S) NRL Report 6556 9b. OTHER REPORT NO(S) (Any other numbers that may be assigned this report)	

10. DISTRIBUTION STATEMENT

Distribution of this document is unlimited.

11. SUPPLEMENTARY NOTES	12. SPONSORING MILITARY ACTIVITY Department of the Navy (Office of Naval Research), Washington, D.C. 20360

13. ABSTRACT

A study was made of the problem of a finite partition function for bound electronic states in a hydrogenic ion and the associated problems of the intensity drop of spectral lines and the lowering of the effective ionization potential. Solutions of the Schrödinger equation (SE) with the complete screened Coulomb potential (CSCP) were obtained for 1s, 2s, 2p, 3s, 3p, and 3d states. The CSCP used is given by

$$V(r) \begin{cases} V_i(r) = -Ze^2\left(\dfrac{1}{r} - \dfrac{1}{D+A}\right), & 0 \leqq r \leqq A \\ V_0(r) = -Ze^2 \dfrac{D}{D+A} \dfrac{\exp[(A-r)/D]}{r}, & r \geqq A \end{cases}$$

where D is the screening radius and A is the mean minimum radius of the ion atmosphere. The standard transformations $x = 2Zr/\lambda a_0$ and $E_\lambda = -Z^2\mu e^4/2\hbar^2\lambda^2$, where λ is the CSCP quantum number, yield the well-known form of the SE with λ in place of n. The numerical solutions of the SE are obtainable using a nonlinear method that is accurate and stable. The resulting quantum numbers can be accurately described by simple analytic fits for a wide range of the interesting values of D. For a given ratio of A to D the relative normalizations of the CSCP wave functions to the corresponding Coulomb wave functions $\Phi_{n,\ell}(\lambda)$ can also be described by simple analytic functions. It was shown that for states where $3a_0n^2/2Z \approx D$, Φ is generally near $1/e$ for solutions with $A = D$. For $3a_0n^2/2Z > D$, Φ decreases rapidly. This Φ-function

(over)

DD FORM 1 NOV 65 1473 (PAGE 1)

S/N 0101-807-6801

Security Classification

Security Classification

14. KEY WORDS	LINK A ROLE	LINK A WT	LINK B ROLE	LINK B WT	LINK C ROLE	LINK C WT
Finite partition function						
Complete Screened Coulomb potential						
Equilibrium probability						
Maximum bound principal quantum number						
Screening radius						
Bound states						
Wave function						
Positive screening						
Negative screening						
Eigenvalue						
Schrödinger equation						
Normalization integral						
Hydrogenic ion						

is used in the definition of a finite electronic partition function as a multiplying factor for each Boltzmann factor, viz., $\Phi_{n,\ell}(\lambda)\exp(-E_\lambda/kT)$. This is shown to be analogous to the definition of the equilibrium probability of a state derived by Tolman in his study of nonisolated systems. The problem of the number of screened Coulomb states was resolved: the CSCP yields as many states as the Coulomb potential. However, with the CSCP, for states with $3a_0n^2/2Z > D$, the separation of the levels is less than the corresponding Coulomb levels, i.e., the density of states near the continuum increases. Removal of ℓ-degeneracy, the question of a maximum bound principal quantum number, and integer quantization of the ground state quantum numbers was discussed. In particular, relative to various calculations of a maximum bound principal quantum number by perturbation and/or variational methods, it was shown that these methods actually calculate the increase in the energies of the states with small n, where $3a_0n^2/2Z < D$, by the amount $\Delta E \approx Ze^2/(D+A)$. Present results also apply to the unsolved problem of the intensity drop of hydrogen lines in the solar atmosphere and in laboratory hydrogen at a low temperature, where the observations are in excellent agreement with the CSCP solutions with $A = D/2$ and the effective screening radius is identified with the radius of the mean atomic volume. It was possible to calculate the observed ionization potential of hydrogen and to give evidence of a screened Coulomb red shift in laboratory spectra.